CALCULATIONS · DESIGN · APPLICATIONS B.3.1

Design calculations for snap fit joints in plastic parts

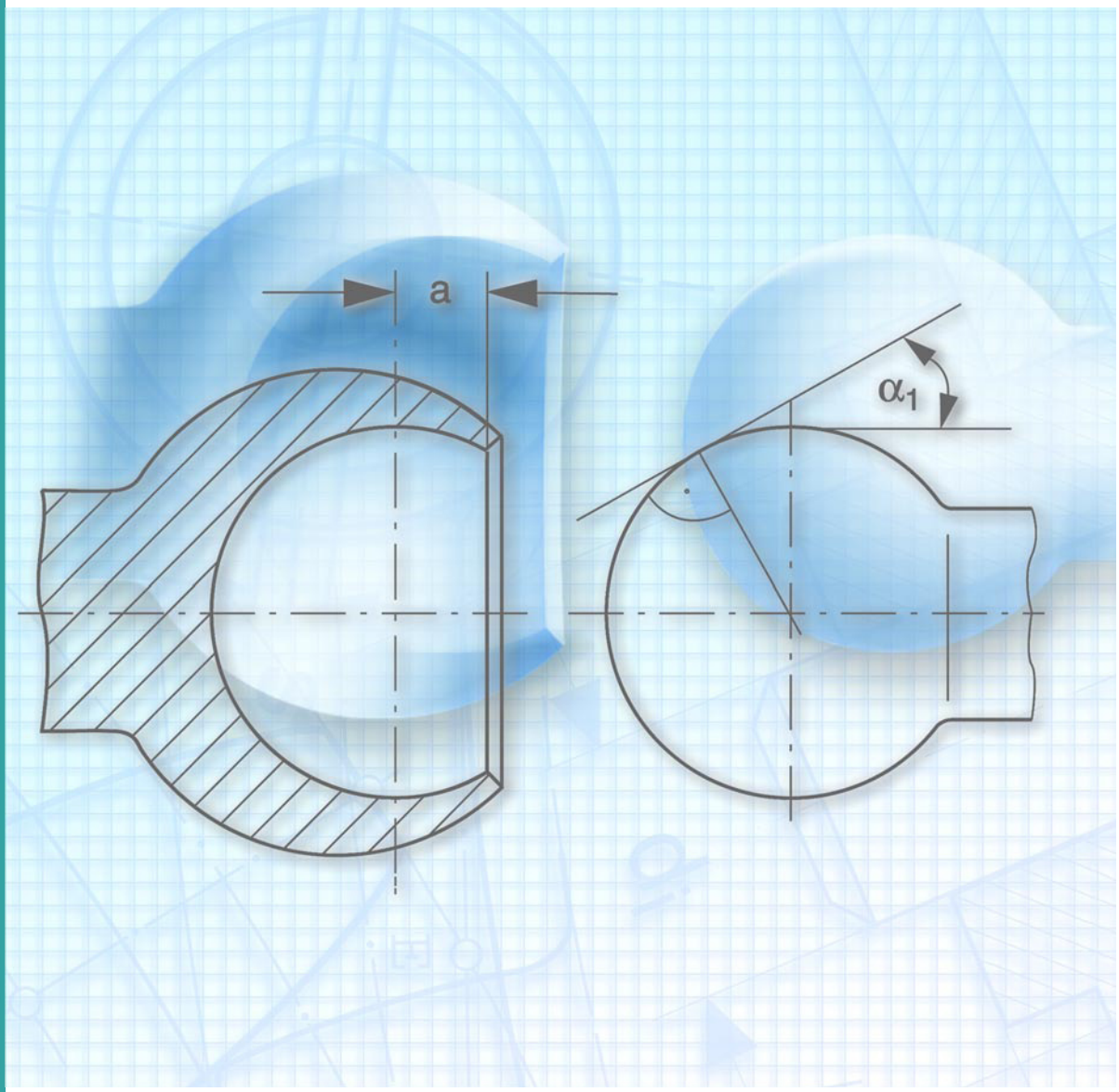

Ticona
Performance Driven Solutions™

Contents

1. *Introduction*

Snap-fits are formfitting joints which permit great design flexibility. All these joints basically involve a projecting lip, thicker section, lugs or barbed legs moulded on one part which engage in a corresponding hole, recess or undercut in the other. During assembly, the parts are elastically deformed. Joints may be non-detachable or detachable, depending on design (figs. 4 and 5). Non-detachable joints can withstand permanent loading even at high temperatures. With detachable joints, it is necessary to test in each individual case the permanent load deformation which can be permitted in the joint. In the unloaded state, snap-fit joints are under little or no stress and are therefore not usually leaktight. By incorporating sealing elements, e.g. O-rings, or by using an adhesive, leaktight joints can also be obtained.

Snap-fits are one of the cheapest methods of joining plastic parts because they are easy to assemble and no additional fastening elements are required.

2. *Requirements for snap-fit joints*

Snap-fits are used to fix two parts together in a certain position. In some cases, it is important to exclude play between the assembled parts (e. g. rattle-free joints for automotive applications). The axial forces to be transmitted are relatively small. In the majority of applications, the joints are not subject to permanent loads (e. g. from internal pressure).

Special fasteners such as rivets and clips also work on the snap-fit principle. They should be easy to insert, suitable for blind fastening, require low assembly force and be able to bridge the tolerances of the mounting hole.

®Hostaform
Acetal copolymer (POM)

®Hostacom
Reinforced polypropylene (PP)

®Celanex
Polybutylene terephthalate (PBT)

®Vandar
Impact-modified
polybutylene terephthalate (PBT-HI)

®Impet
Polyethylene terephthalate (PET)

® = registered trademark

3. *Basic types of snap-fit joint*

The parts with an undercut can be cylindrical, spherical or barbed. There are three corresponding types of snap-fit joint:

1. Barbed leg snap-fit
2. Cylindrical snap-fit
3. Ball and socket snap-fit

3.1 Barbed leg snap-fit

Fig. 1

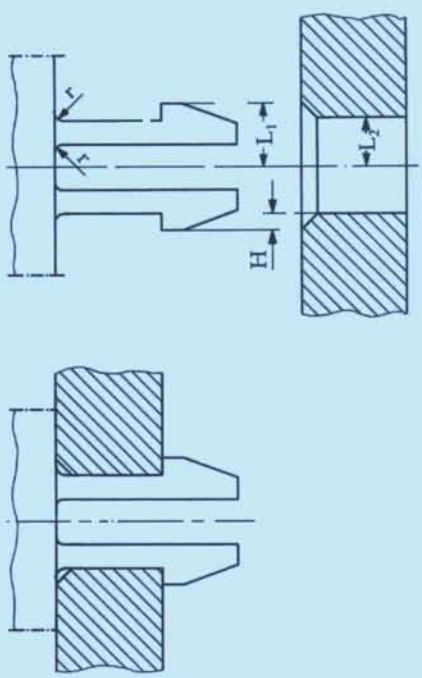

Barbed legs are spring elements supported on one or both sides and usually pressed through holes in the mating part (fig. 1). The hole can be rectangular, circular or a slot. The cross-section of the barbed leg is usually rectangular, but shapes based on round cross-sections are also used. Here, the originally cylindrical snap-fit is divided by one or several slots to reduce dimensional rigidity and hence assembly force (fig. 2).

Fig.2

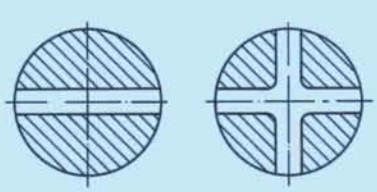

The undercut depth H is the difference between the outside edge of the barb and the inside edge of the hole (fig. 1):

$$\text{undercut depth } H = L_1 - L_2 \qquad (1)$$

The leg is deflected by this amount during assembly.

In designing a barbed leg, care should be taken to prevent overstressing at the vulnerable point of support because of the notch effect. The radius r (fig. 1) should therefore be as large as possible.

3.2 Barbed leg snap-fit supported on both sides

Fig. 3

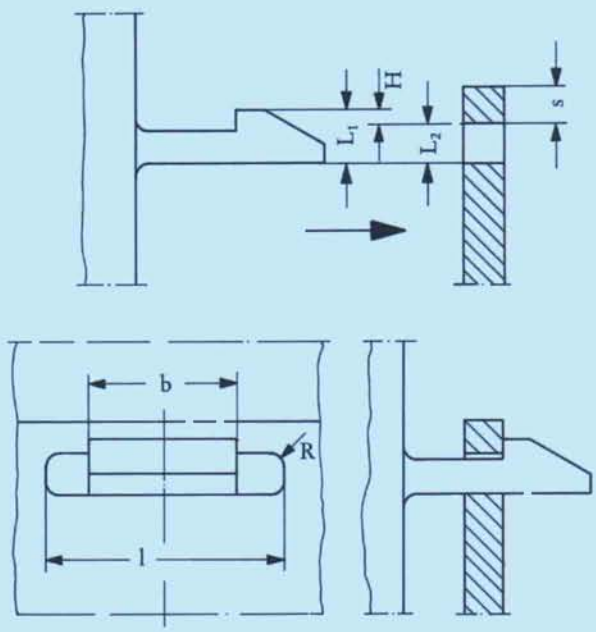

This joint employs a barbed spring element supported on both sides. The undercut depth H is the difference between the outside edge of the barb and the width of the receiving hole (fig. 3). Hence as in formula (1) we obtain:

$$\text{undercut depth } H = L_1 - L_2 \qquad (1a)$$

This snap-joint may be detachable or non-detachable depending on the design of the retaining angle.

3.3 Cylindrical snap-fit

Cylindrical snap-fits consist of cylindrical parts with a moulded lip or thick section which engage in a corresponding groove, or sometimes just a simple hole in the mating part.

Fig. 4: Non-detachable joint

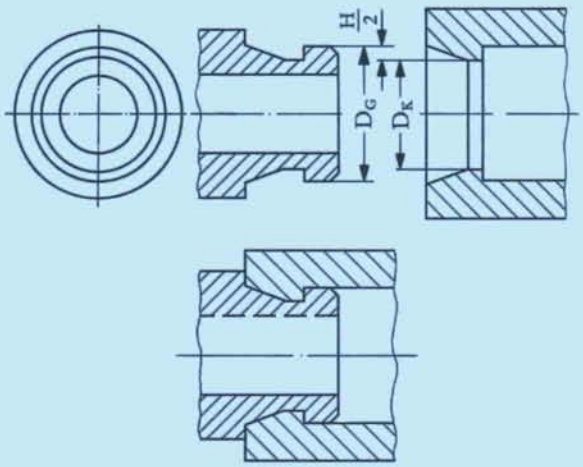

Fig. 5: Detachable joint

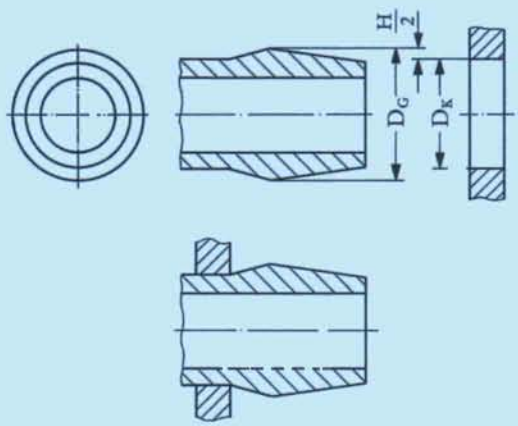

The difference between the largest diameter of the shaft D_G and the smallest diameter of the hub D_K is the undercut depth H.

$$\text{undercut depth } H = D_G - D_K \qquad (2)$$

D_G largest diameter of the shaft [mm]
D_K smallest diameter of the hub [mm]

The parts are deformed by the amount of this undercut depth during assembly. The diameter of the shaft is reduced by $-\Delta D_G$, and the diameter of the hub increased by $+\Delta D_K$.

So the undercut depth can also be described as

$$H = \Delta D_G + \Delta D_K \qquad (3)$$

As a result of these diameter changes, the shaft and hub are deformed as follows:

compression (–) of the shaft

$$\varepsilon_1 = -\frac{\Delta D_G}{D_G} \cdot 100\% \qquad (4)$$

elongation (+) of the hub

$$\varepsilon_2 = +\frac{\Delta D_K}{D_K} \cdot 100\% \qquad (5)$$

As it is not known how the undercut depth H is apportioned between the mating parts, it is assumed for simplicity that only one part undergoes a deformation ε corresponding to the whole undercut depth H.

$$\varepsilon = \frac{H}{D_G} \cdot 100\% \quad \text{or} \quad \varepsilon = \frac{\Delta D_K}{D_K} \cdot 100\% \qquad (6)$$

3.4 Ball and socket snap-fit

Fig. 6

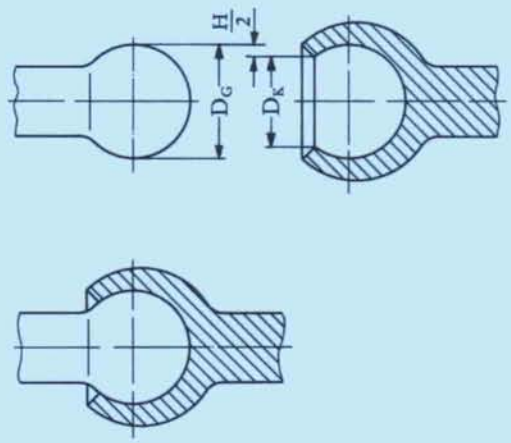

Ball and socket snap-fits (fig. 6) are mainly used as motion transmitting joints. A ball or ball section engages in a corresponding socket; the undercut depth H is the difference between the ball diameter D_G and the socket opening diameter D_K.

$$\text{undercut depth } H = D_G - D_K \qquad (7)$$

D_G ball diameter [mm]
D_K socket opening diameter [mm]

Because the shaft is solid and therefore very rigid, the hole undercut depth H must be overcome by expanding the hub. As a result of this diameter change, the hub is deformed as follows:

$$\text{elongation } \varepsilon = \frac{D_G - D_K}{D_K} \cdot 100\% = \frac{H}{D_K} \cdot 100\% \qquad (8)$$

4. *Critical dimensions for a snap-fit joint*

Irrespective of the type of snap-fit there is a linear relation between the undercut depth H and elongation ε. The maximum permissible undercut depth $H_{max.}$ is limited by the specified maximum permissible elongation $\varepsilon_{max.}$.

The load-carrying capacity of snap-fits depends on the elastic modulus E and coefficient of friction μ. It can be matched to the requirements of the joint by adjusting undercut depth H and assembly angle α_1 or retaining angle α_2 (see section 4.4).

4.1 Maximum permissible undercut depth $H_{max.}$ and maximum permissible elongation $\varepsilon_{max.}$

In barbed legs (fig. 7), the following relation applies between undercut depth H (= deflection) as a result of deflection force F_B and elongation or compression in the outer fibre region of the barbed leg cross-section (rectangular section):

$$\text{undercut depth } H_{max.} = \frac{2}{3} \cdot \frac{l^2}{h} \cdot \frac{\varepsilon_{max.}}{100} \qquad (9)$$

l	barbed leg length	[mm]
h	barbed leg height	[mm]
$\varepsilon_{max.}$	permissible elongation	[%]

Fig. 7

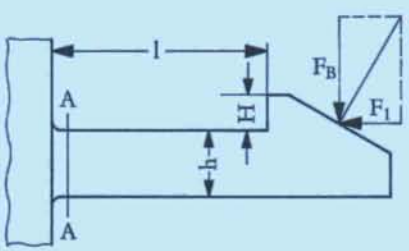

Fig. 8: Elongation in cross-section A – A (fig.7)

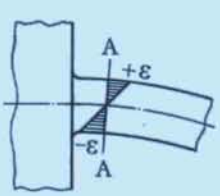

The maximum deformation (fig. 8) only applies in the critical region A – A, fig. 7, while in other cross-sections the deformation is lower. So barbed legs are stressed much less than cylindrical snap-fits. As a result of this, higher elongation is permissible and in many cases is necessary for design reasons.

For non-rectangular barbed leg cross-sections, the following relationships apply between undercut depth H and deformation ε in the outer fibre region (outer fibre elongation):


semicircular cross-section

$$H_{max.} = 0.578 \frac{l^2}{r} \cdot \frac{\varepsilon_{max.}}{100} \qquad (10)$$


third of a circle cross-section

$$H_{max.} = 0.580 \frac{l^2}{r} \cdot \frac{\varepsilon_{max.}}{100} \qquad (11)$$


quarter of a circle cross-section

$$H_{max.} = 0.555 \frac{l^2}{r} \cdot \frac{\varepsilon_{max.}}{100} \qquad (12)$$


These relationships also apply approximately to leg cross-sections in the form of sectors of an annulus.

A comparison between formula 9 and formulae 10 to 12 shows that the maximum permissible undercut depth $H_{max.}$ for barbed legs with cross-sections in the form of segments of a circle is 15% lower than that of a rectangular barbed leg cross-section (assumption: h = r).

The maximum permissible undercut depth $H_{max.}$ for barbed legs of different length and height with a rectangular cross-section can be read off figs. 10 to 13.

Fig. 9

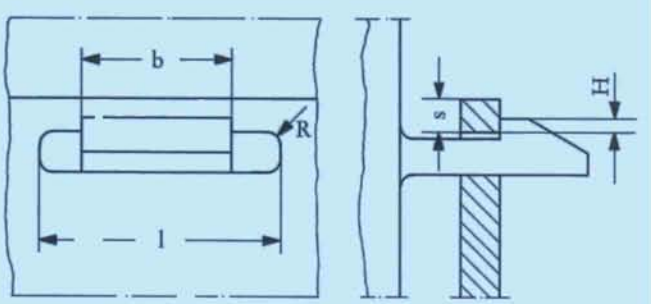

The maximum permissible undercut depth $H_{max.}$ for barbed leg snap-fits supported on both sides can be calculated with the aid of fig. 14, irrespective of the material. Fig. 14 applies for $\varepsilon_{max.}$ = 6% (see calculation example 6.4).

Fig. 10: Maximum permissible undercut depth $H_{max.}$ for Hostaform and Hostalen PP

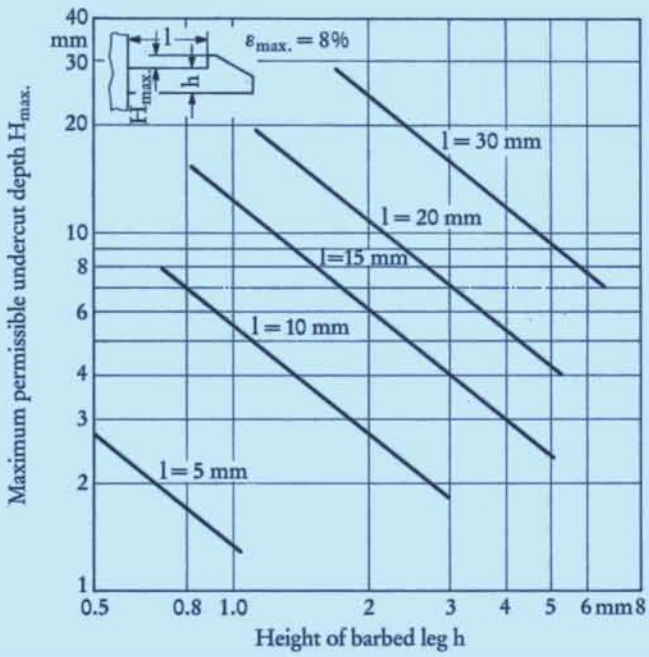

Fig. 11: Maximum permissible undercut depth $H_{max.}$ for Hostaform C 9021 GV 1/30

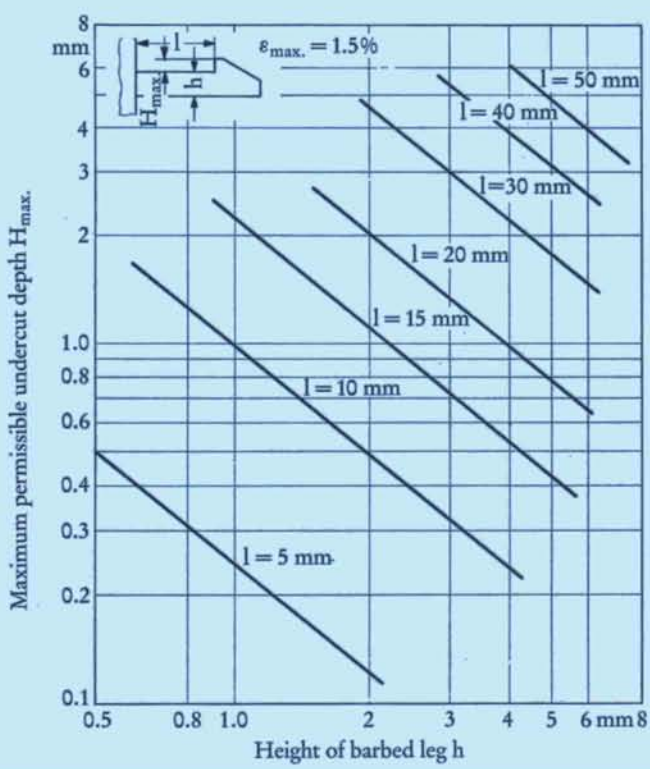

Fig. 12: Maximum permissible undercut depth $H_{max.}$ for Hostacom M 4 N01 and G 3 N01

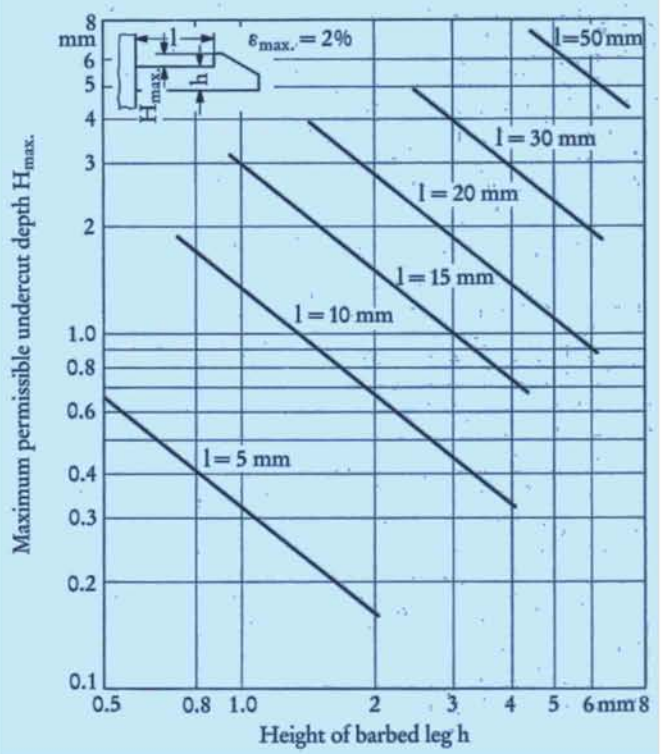

Fig. 13: Maximum permissible undercut depth $H_{max.}$ for Hostacom G 2 N01 and M 2 N01

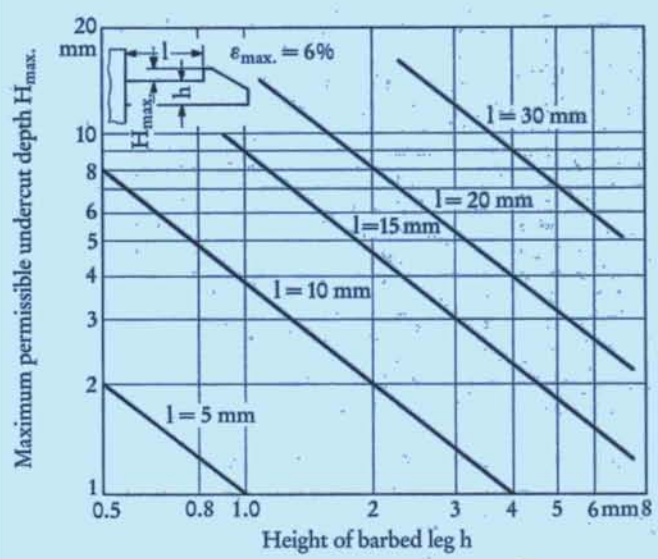

The undercut depth H is calculated as follows:

$$H_{max.} = \frac{1}{12} \cdot \frac{l^2}{s} \cdot \frac{\left(1-\frac{b}{l}\right)^2 \cdot \left(1+3\frac{b}{l}\right)}{\left(1+\frac{b}{l}\right)} \cdot \frac{\varepsilon_{max.}}{100} \text{ [mm]} \quad (13)$$

b barb width [mm]
l length of hole [mm]
s thickness of leg [mm]
$\varepsilon_{max.}$ maximum permissible elongation (table 1) [%]

Fig. 14: Barbed leg snap-fit supported on both sides; relative undercut depth $\frac{H}{l}$ as a function of barb width and spring leg thickness for $\varepsilon_{max.} = 6\%$

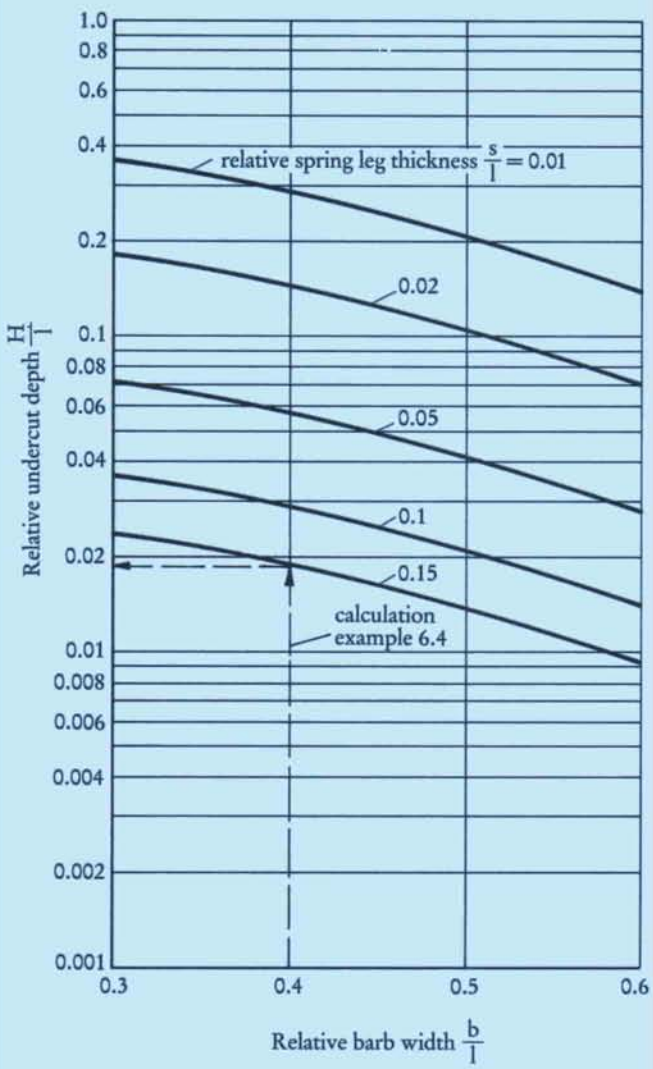

With cylindrical snap-fits and ball and socket snap-fits, the maximum permissible undercut depth can be calculated from the maximum permissible elongation $\varepsilon_{max.}$ (%) using the formula:

maximum permissible undercut depth (14)

$$H_{max.} = \frac{\varepsilon_{max.}}{100} \cdot D_G$$

D_G outside diameter of the shaft [mm] in cylindrical snap-fits or ball diameter [mm] in ball and socket snap-fits

The maximum permissible elongation of materials with a definite yield point (e. g. Hostaform) should be about a third of the elongation at yield stress ε_s (fig. 15a). For materials without a definite yield point (e. g. glass fibre reinforced Hostacom, fig. 15b), the maximum permissible elongation (see table 1) should be about a third of the elongation at break ε_R.

Fig. 15a: For materials with a definite yield point σ_s (e. g. Hostaform)

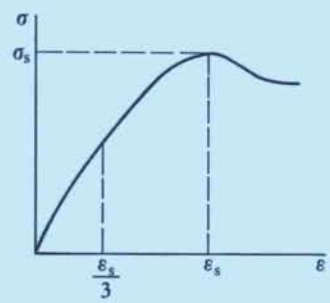

Fig. 15b: For materials without a definite yield point σ_s (e. g. Hostacom)

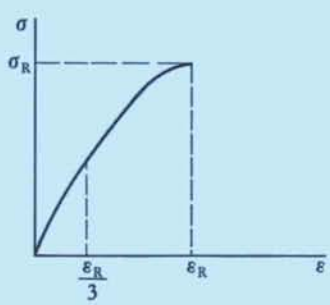

Fig. 16

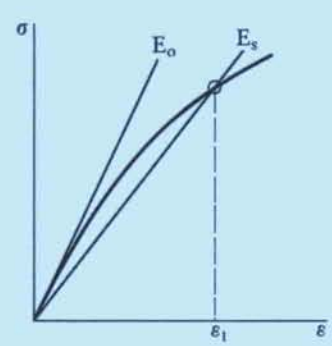

Table 1:
Maximum permissible elongation $\varepsilon_{max.}$ for determination of the maximum permissible undercut depth $H_{max.}$

Material	Maximum permissible elongation $\varepsilon_{max.}$ (%)	
	Barbed leg	Cylindrical snap-fits, ball and socket snap-fits
Hostaform C 52021 Hostaform C 27021 Hostaform C 13021 Hostaform C 13031 Hostaform C 9021 Hostaform C 2521 Hostaform C 9021 K Hostaform C 9021 M Hostaform C 9021 TF Hostaform T 1020 Hostaform S 9063/S 27063	8	4
Hostaform C 9021 GV 1/30	1.5	0.8
Hostaform S 9064/S 27064	10	6
Hostacom M2 N02 Hostacom M2 N01 Hostacom G2 N01	6	3
Hostacom M4 N01 Hostacom G2 N02 Hostacom M1 U01	2	1
Hostacom G3 N01 Hostacom M4 U01	1.5	1.0
Impet 2600 GV 1/30	≦ 1.0	≦ 0.5
Vandar 4602 Z	≦ 3.0	≦ 2.0
Celanex 2500	≦ 2.0	≦ 1.0
Celanex 2300 GV 1/30 Celanex 2300 GV 3/30	≦ 1.0	≦ 0.5

4.2 *Elastic modulus E*

The elastic modulus E_0 is defined in DIN 53 457 as the slope of the tangent to the stress-strain curve at the origin (fig. 16, page 8).

$$E_0 = \frac{\sigma}{\varepsilon} \quad \text{at the point } \varepsilon = 0 \qquad (15)$$

With greater elongation, e. g. ε_1 (fig. 16), the elastic modulus is smaller because of the deviation from linearity between σ and ε. The elastic modulus then corresponds to the slope of a secant which is drawn from the origin through the ε_1 point of the stress strain curve. This is known as secant modulus E_s and is dependent on the magnitude of elongation ε.

The following applies:

$$E_S = f(\varepsilon) \qquad (16)$$

This secant modulus E_S is used in design calculations for snap-fits. Fig. 17 plots the secant modulus against elongation ε up to the maximum permissible elongation for barbed legs.

4.3 *Coefficient of friction μ*

In assembling snap-fits, friction has to be overcome. The degree of friction depends on the materials used for the mating elements, surface roughness and surface loading. Table 2 gives coefficient of friction ranges for various combinations of mating element materials. The friction values quoted are guide values only.

Table 2

Mating element materials	Coefficient of friction μ
Hostaform/Hostaform	0.2 to 0.3
Hostaform/other plastics	0.2 to 0.3
Hostaform/steel	0.1 to 0.2
Hostacom/Hostacom	0.4
Hostacom/other plastics	0.3 to 0.4
Hostacom/steel	0.2 to 0.3
Impet/Impet	0.2 to 0.3
Impet/other plastics	0.2 to 0.3
Impet/steel	0.1 to 0.2
Vandar/Vandar	0.3 to 0.4
Vandar/other plastics	0.2 to 0.3
Vandar/steel	0.2 to 0.3
Celanex/Celanex	0.2 to 0.3
Celanex/other plastics	0.2 to 0.3
Celanex/steel	0.1 to 0.2

Fig. 17: Secant modulus E_S as a function of outer fibre elongation (based on 3-point flexural test) ($\dot{\varepsilon} \approx 1\%/\text{min}$)

a Celanex 2300 GV 1/30
b Hostaform C 9021 GV 1/30
c Hostacom G 3 N01
d Hostacom M 4 N01
e Hostaform C 9021
f Celanex 2500
g Hostacom M 2 N01
h Hostacom G 2 N01
i Vandar 4602 Z

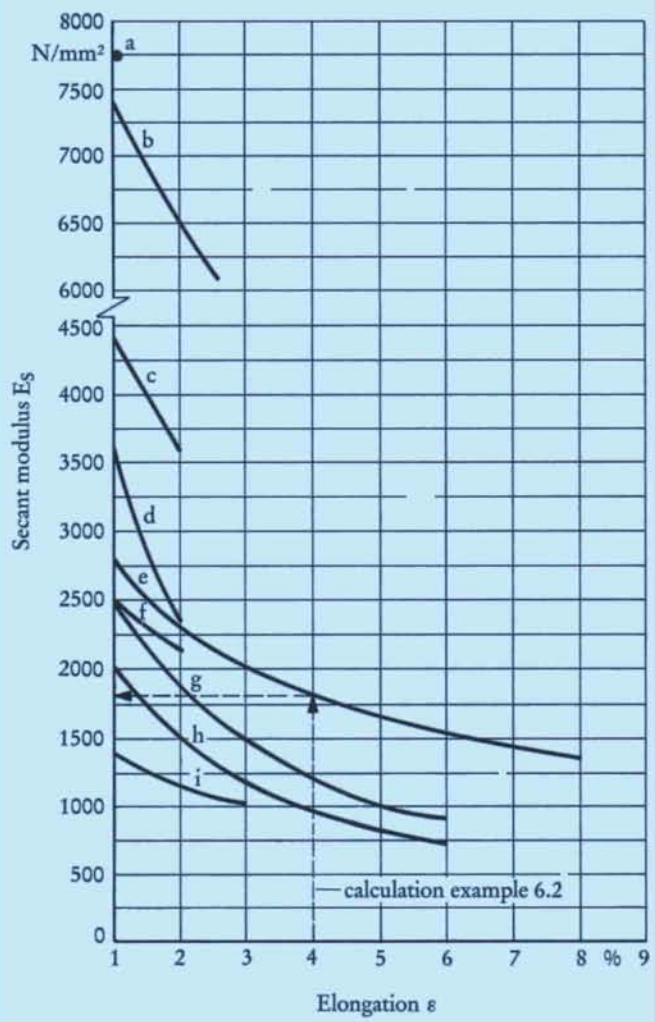

4.4 *Assembly angle α_1 and retaining angle α_2*

The assembly angle α_1 (figs. 18 and 19), along with the barb dimensions and coefficient of friction μ between the mating elements (table 2), determines the required assembly force F_1 (fig. 20). The greater α_1 the higher the assembly force required. With a large assembly angle ($\alpha_1 \geqq 45°$) and high coefficient of friction μ, it may no longer be possible for parts to be assembled. The barb then shears off rather than being deflected. The recommended assembly angle for barbed legs and cylindrical snap-fits is $\alpha_1 = 15$ to $30°$.

With ball and socket snap-fits, the assembly angle cannot be freely chosen. It depends on the maximum permissible socket opening diameter D_K (fig. 27).

The retaining angle α_2 (figs. 18 and 19) decides how much loading the joint can stand. The maximum load-bearing capacity is reached when the retaining angle is $\alpha_2 = 90°$ (fig. 19). During long-term loading and/or in the event of elevated ambient temperatures, the retaining angle α_2 should always be 90°. The joint is then permanent. For detachable joints, a retaining angle $\alpha_2 \leqq 45°$ should be provided, preferably $\alpha_2 = 30$ to $45°$.

Fig. 18: Detachable joint

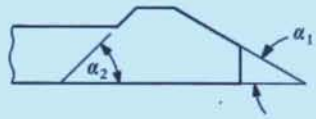

Fig. 19: Non-detachable joint for $\alpha_2 = 90°$

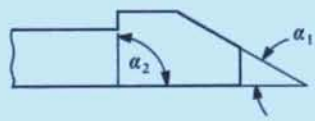

Fig. 20

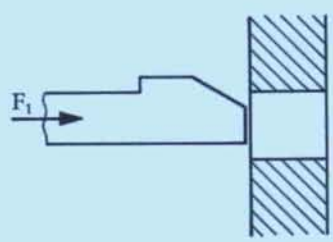

F_1 = assembly force required

5. *Design calculations for snap-fit joints*

The load-bearing capacity of snap-fits under steady (short-term) stress depends primarily on:

1. the mechanical properties of the plastics concerned, particularly stiffness as expressed by the elastic modulus E_S,

2. the design of the snap-fit, i. e. wall thickness, undercut depth H, retaining angle α_2.

Load-bearing capacity is defined as the pull-out force F_2 which the joint can stand in the opposite direction to assembly without the parts separating.

In many cases, it is possible to design the direction of snap-fit assembly at right angles to the actual loading direction F during service (fig. 21). Then the load-bearing capacity of the joint is not determined by pull-out force F_2 but by the break resistance or shear strength of the vulnerable cross-section. This design technique is most often used with ball and socket snap-fits.

Fig. 21

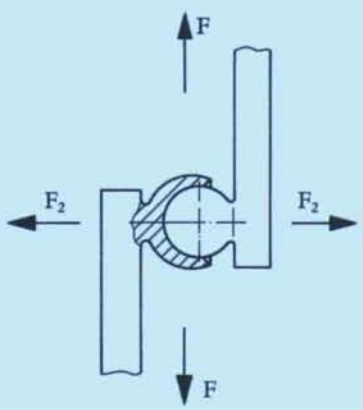

Table 3

Barbed leg cross-section		Moment of inertia [mm⁴]	
rectangle		$\frac{b \cdot h^3}{12}$ where	b leg width [mm] h leg height [mm]
semicircle		$0.110\ r^4$	r radius [mm]
third of a circle		$0.0522\ r^4$	
quarter of a circle		$0.0508\ r^4$	

5.1 *Barbed leg snap-fit*

Fig. 22

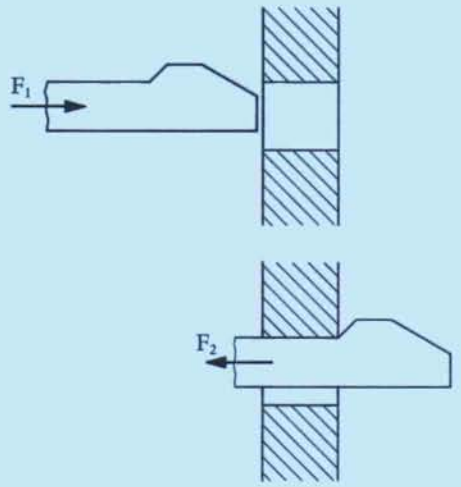

The assembly force F_1 and pull-out force F_2 (fig. 22) for barbed legs can be calculated from the formula:

$$F_{1,2} = \frac{3H \cdot E_S \cdot J}{l^3} \cdot \frac{\mu + \tan \alpha_{1,2}}{1 - \mu \cdot \tan \alpha_{1,2}} \text{ [N]} \qquad (17)$$

H	undercut depth	[mm]
E_S	secant modulus	[N/mm²] (Fig. 17)
J	moment of inertia	[mm⁴] (table 3)
l	barbed leg length	[mm]
μ	coefficient of friction	(table 2)
α_1	assembly angle	[°]
α_2	retaining angle	[°]

The factor $\frac{\mu + \tan \alpha_{1,2}}{1 - \mu \cdot \tan \alpha_{1,2}}$ can be taken directly from fig. 23.

Fig. 23: Factor $\frac{\mu + \tan \alpha_{1,2}}{1 - \mu \cdot \tan \alpha_{1,2}}$ (from formulae 17, 22 and 25) as a function of assembly/retaining angle $\alpha_{1,2}$

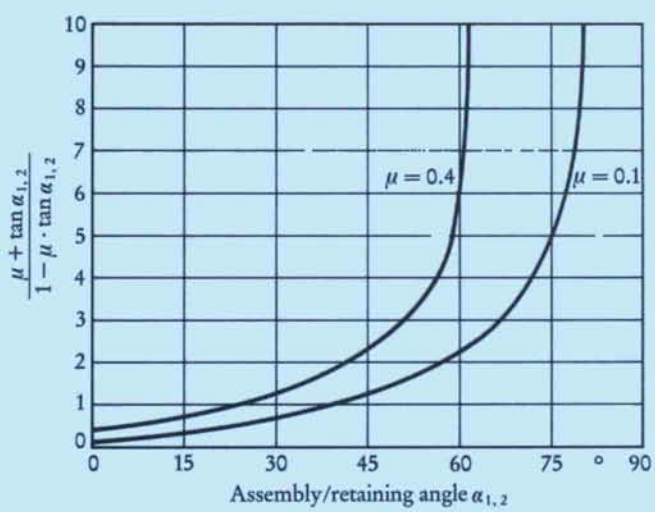

With the retaining angle $\alpha_2 = 90°$, the pull-out force F_2 is determined by the shear-stressed area and the shear strength τ_B of the plastic used.

Table 4

Material	Ultimate tensile strength σ_R and tensile strength σ_B [N/mm²]*
Hostaform C 52021	65
Hostaform C 27021	64
Hostaform C 13021	65
Hostaform C 13031	71
Hostaform C 9021	64
Hostaform C 2521	62
Hostaform C 9021 K	62
Hostaform C 9021 M	64
Hostaform C 9021 TF	49
Hostaform T 1020	64
Hostaform C 9021 GV 1/30	110
Hostaform S 27063	50
Hostaform S 9063	53
Hostaform S 27064	42
Hostaform S 9064	42
Hostacom M2 N02	19
Hostacom M2 N01	33
Hostacom M4 N01	33
Hostacom G2 N01	32
Hostacom G2 N02	70
Hostacom G3 N01	80
Hostacom M1 U01	36
Hostacom M4 U01	33
Celanex 2500	65
Celanex 2300 GV 1/30	150
Celanex 2300 GV 3/30	50
Vandar 4602 Z	40
Impet 2600 GV 1/30	165

*) Test specimen injection moulded according to DIN 16770 part 2.

Fig. 24

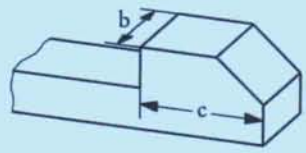

The shear stress τ_s is

$$\tau_s = \frac{F_2}{b \cdot c} \text{ [N/mm²]} \quad (18)$$

Taking into account ultimate tensile strength σ_R or tensile strength σ_B (table 4), the following holds true for shear strength

$$\tau_B = 0.6 \cdot \sigma_R \quad (19)$$

$$\text{or } \tau_B = 0.6 \cdot \sigma_B \quad (20)$$

$$F_{2max.} = A \cdot \tau_B = b \cdot c \cdot \tau_B \text{ [N]} \quad (21)$$

5.2 *Cylindrical snap-fit*

Fig. 25

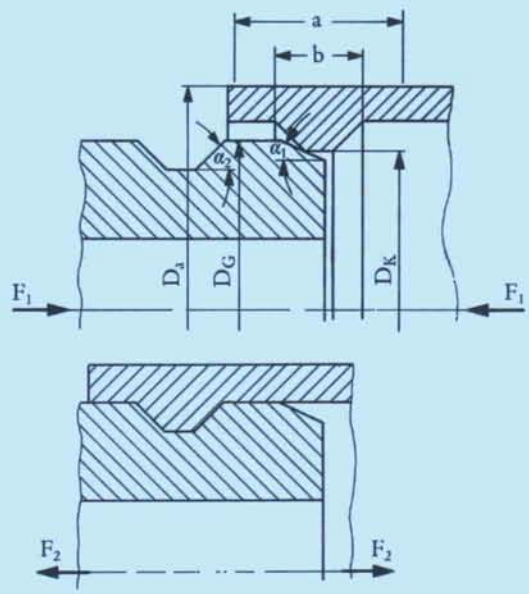

The assembly force F_1 and pull-out force F_2 for cylindrical snap-fits – unlike for barbed legs – can only be roughly estimated. This is because the length a (fig. 25) which is deformed during assembly of the parts with consequent increase in assembly force F_1 is unknown. The length a depends on both the wall thickness of the hub and the undercut depth H. A useful guide to a has proved to be twice the width b of the moulded lip.

The assembly force F_1 and pull-out force F_2 can be calculated from the formula:

$$F_{1,2} = p \cdot \pi \cdot D_G \cdot 2b \frac{\mu + \tan \alpha_{1,2}}{1 - \mu \cdot \tan \alpha_{1,2}} \text{ [N]} \quad (22)$$

p joint pressure [N/mm²]
D_G outside diameter of the hub [mm]
b width of the moulded lip [mm]
μ coefficient of friction (table 2)
α_1 assembly angle [°]
α_2 retaining angle [°]

Between undercut depth H and joint pressure p, the following relationship applies:

$$p = \frac{H}{D_K} \cdot E_S \cdot \frac{1}{K} \text{ [N/mm²]} \quad (23)$$

D_K smallest diameter of the hub [mm]

The geometry factor K depends on the dimensions of the snap-fit:

$$K = \frac{\left(\frac{D_a}{D_G}\right)^2 + 1}{\left(\frac{D_a}{D_G}\right)^2 - 1} + 1 \quad (24)$$

D_a outside diameter of the hub [mm]
D_G outside diameter of the shaft [mm]

Here it is assumed that the whole undercut depth H is accommodated by expansion of the hub. With thin-walled shafts, the shaft deforms as well but this can be ignored in the case described here. Fig. 26 shows the geometry factor K as a function of the diameter ratio D_a/D_G.

5.3 *Ball and socket snap-fit*

In this design (fig. 27), the assembly angle α_1 and retaining angle α_2 and hence assembly force F_1 and pull-out force F_2 are the same.

The assembly/retaining angle is between 8° ($\varepsilon = 1\%$) and 16° ($\varepsilon = 4\%$), depending on elongation.

Fig. 26: Geometry factor K as a function of diameter ratio $\frac{D_a}{D_G}$ or $\frac{D_G}{D_K}$

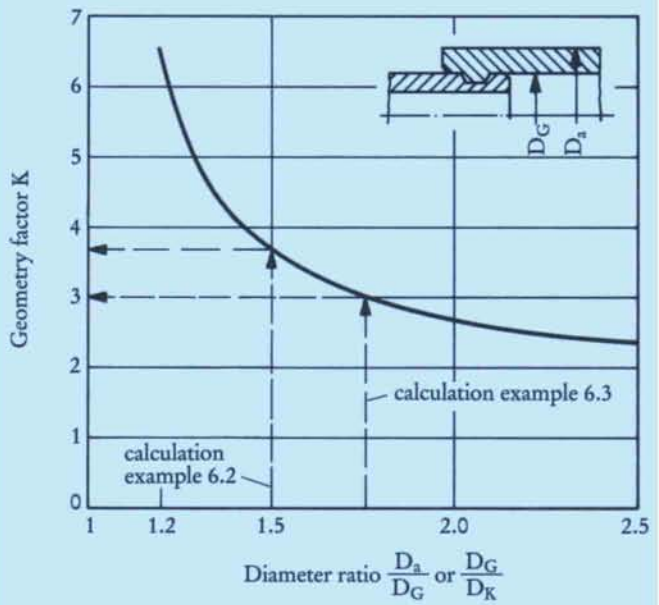

Fig. 27

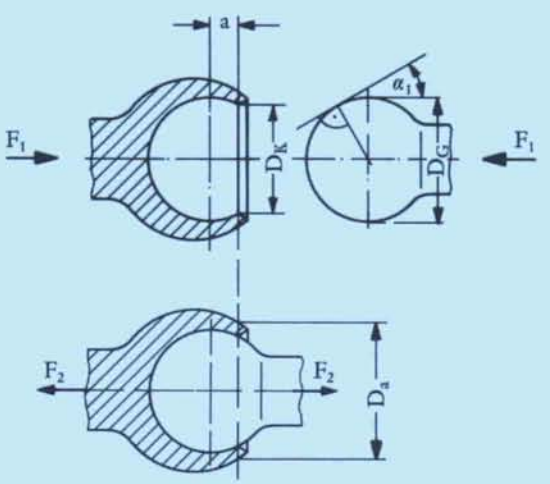

Table 5

$\varepsilon = \frac{H}{D_K} \cdot 100\%$	Assembly angle α_1 Retaining angle α_2	$\frac{a}{D_G}$
1	8°	0.07
2	11.4°	0.10
3	13.9°	0.12
4	15.9°	0.14

To estimate assembly or pull-out force, the formulae for cylindrical snap-fits are used:

$$F_1 = F_2 = p \cdot \pi \cdot D_G^2 \cdot \frac{a}{D_G} \cdot \frac{\mu + \tan \alpha}{1 - \mu \cdot \tan \alpha} \quad [N] \qquad (25)$$

p joint pressure [N/mm²]
D_G ball diameter [mm]
$\frac{a}{D_G}$ deformation length divided by the ball diameter (table 5)
μ coefficient of friction (table 2)
α assembly or retaining angle [°] (table 5)

The relationship between undercut depth H and joint pressure p can be described by the following formula (23):

$$p = \frac{H}{D_K} \cdot E_S \cdot \frac{1}{K} \quad [N/mm^2]$$

H undercut depth [mm]
D_K socket opening diameter [mm]
E_S secant modulus [N/mm²] (fig. 17)
K geometry factor

$$K = \frac{\left(\frac{D_a}{D_K}\right)^2 + 1}{\left(\frac{D_a}{D_K}\right)^2 - 1} + 1 \qquad (26)$$

6. *Calculation examples*

6.1 Barbed leg snap-fit

The top and bottom plates of a time switch are to be detachably joined by two diagonally opposite spacers and two barbed legs. The hole diameter in the top plate is $D_K = 8$ mm. The pull-out force F_2 required per barbed leg is 50 N. The barbed legs are to be injection moulded from Hostaform C 9021 and will have a slotted circular cross-section (fig. 28).

Fig. 28

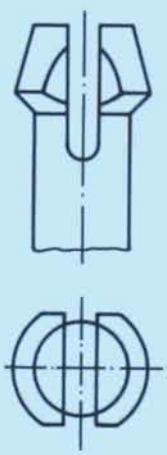

a) What should the dimensions of the barbed leg be?
b) What assembly force F_1 is required?
c) What pull-out force F_2 is obtained?

a) The maximum permissible outer fibre elongation is chosen to be $\varepsilon_{max.} = 1\%$. For the semicircular cross-section, the following applies using formula (10):

$$H = 0.578 \cdot \frac{l^2}{r} \cdot \varepsilon_{max.}$$

$$r = \frac{D_K}{2} = 4 \text{ mm}$$

l is chosen to be 15 mm

$$H = 0.578 \cdot \frac{15^2}{4} \cdot 0.01$$

$$H = 0.3 \text{ mm}$$

The diameter of the undercut is calculated from $D_K + 2H = 8.6$ mm. The slot width is chosen to be 1 mm, the assembly angle α_1 30° and the retaining angle α_2 45°.

b) Assembly force F_1

For the assembly force F_1 formula (17) applies:

$$F_1 = \frac{3H \cdot E_S \cdot J}{l^3} \cdot \frac{\mu + \tan\alpha_1}{1 - \mu \cdot \tan\alpha_1}$$

$H = 0.3$ mm
$E_S = 2800$ N/mm² (fig. 17).

For the Hostaform/steel mating elements, it is assumed that the friction coefficient $\mu = 0.2$ (table 2).

Using table 3 we obtain for the semicircular cross section:

$$J = 0.110\, r^4 = 0.11 \cdot 4^4 = 28.2 \text{ mm}^4$$

So assembly force F_1 works out as

$$F_1 = \frac{3 \cdot 0.3 \cdot 2800 \cdot 28.2}{15^3} \cdot \frac{0.2 + 0.577}{1 - 0.2 \cdot 0.577}$$

$$\underline{F_1 = 18.5 \text{ N}}$$

Each securing element comprises two barbed legs which each have to be deflected by H. The assembly force per element is therefore $2 \cdot F_1 = 37$ N.

c) Pull-out force F_2

The pull-out force F_2 is calculated in the same way as assembly force except that $\alpha_2 = 45°$ is substituted for α_1. The pull-out force is thus

$$\underline{F_2 = 31.6 \text{ N}}$$

Each element withstands a pull-out force of $2 \cdot 31.6 \text{ N} \approx 63$ N, which is greater than the required pull-out force of 50 N.

6.2 Cylindrical snap-fit

The body of a rubber-tyred roller is to be made in two parts which are permanently joined together (fig. 29). Because of the relatively high stress involved and the fact that the roller bears directly onto a steel axle, Hostaform is used as the construction material.

a) What should the dimensions of the snap-fit be (undercut depth H)?
b) What assembly force F_1 is required?
c) What is the pull-out force F_2?

a) Maximum permissible undercut depth $H_{max.}$

To determine the maximum permissible undercut depth $H_{max.}$, it is assumed that only the hub is deformed. The greatest elongation takes place at the diameter D_K which is expanded during assembly to $D_G = 16$ mm. The maximum permissible elongation for Hostaform is $\varepsilon_{max.} = 4\%$, according to table 1.

Fig. 29

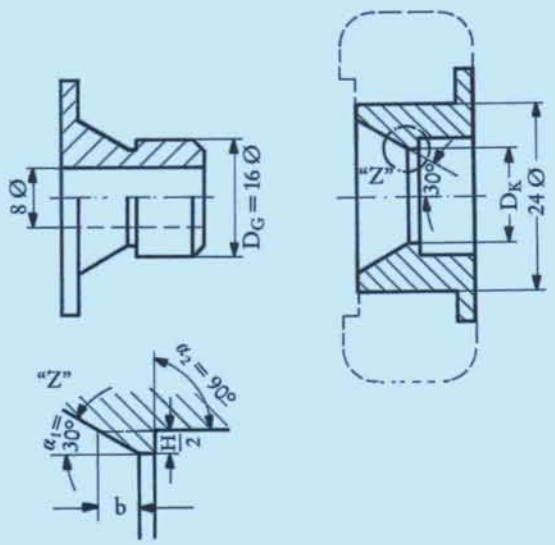

So the maximum permissible undercut depth can be calculated according to Formula (14):

$$H_{max.} = \frac{\varepsilon_{max.}}{100} \cdot D_G$$

$$= \frac{4}{100} \cdot 16$$

$$\underline{H_{max.} = 0.64 \text{ mm}}$$

$$D_K = D_G - H$$
$$= 16 - 0.64$$
$$D_K = 15.36 \text{ mm}$$

The diameter D_K is chosen to be 15.4 mm.

b) Required assembly force F_1

For the assembly force F_1, formula (22) applies:

$$F_1 = p \cdot \pi \cdot D_G \cdot 2b \, \frac{\mu + \tan \alpha_1}{1 - \mu \cdot \tan \alpha_1}$$

The assembly angle α_1 is 30°. The coefficient of friction for Hostaform/Hostaform mating elements is asumed to be $\mu = 0.2$ (table 2). The width b of the undercut can be determined from the assembly angle α_1 and the undercut depth H.

$$b = \frac{H}{2 \cdot \tan \alpha_1}$$

$$= \frac{H}{2 \cdot \tan 30°}$$

$$= \frac{0.64}{2 \cdot 0.577}$$

$$b = 0.55 \text{ mm}$$

The joint pressure p is calculated from formula (23).

$$p = \frac{H}{D_K} \cdot E_S \cdot \frac{1}{K}$$

With $\frac{D_a}{D_G} = \frac{24}{16} = 1.5$ fig. 26 shows a value for K of 3.6.

The secant modulus for $\varepsilon_{max.} = 4\%$ for Hostaform (fig. 17) is $E_S = 1800$ N/mm².

So the joint pressure works out as

$$p = 0.04 \cdot \frac{1800}{3.6}$$

$$p = 20 \text{ N/mm}^2$$

The assembly force F_1 is

$$F_1 = 20 \cdot \pi \cdot 16 \cdot 2 \cdot 0.55 \, \frac{0.2 + 0.577}{1 - 0.2 \cdot 0.577}$$

$$\underline{F_1 = 970.8 \text{ N}}$$

c) Pull-out force F_2

Because the retaining angle $\alpha_2 = 90°$, the joint is permanent. The force required to separate the mating elements can be calculated from the shear strength τ_B and the shear-stressed area A (shear surface).

According to formula (20) the shear strength is

$$\tau_B = 0.6 \cdot \sigma_B$$

$\sigma_B = 62$ N/mm² e.g. for Hostaform C 2521 (table 4)

$$\tau_B = 0.6 \cdot 62$$

$$\tau_B = 37.2 \text{ N/mm}^2$$

The shear surface in this case is

$$A = \pi \cdot D_G \cdot b$$
$$= \pi \cdot 16 \cdot 0.55$$
$$A = 27.6 \text{ mm}^2$$

So using formula (21), the pull-put force ist:

$$F_{2\,max.} = A \cdot \tau_B$$
$$= 27.6 \cdot 37.2$$
$$\underline{F_{2\,max.} = 1027\ N}$$

6.3 *Ball and socket snap-fit*

In a car, the movement of the accelerator pedal is transmitted via a linkage to the carburettor. A ball and socket joint connecting the pedal to the linkage (fig. 30) and made from Hostacom G 3 N 01 is required to have a pull-out force F_2 of at least 100 N. The ball diameter $D_G = 8$ mm, the outside diameter $D_a = 14$ mm.

Fig. 30

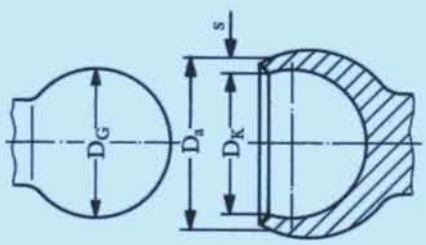

a) How large should the socket opening diameter D_K be?

b) What assembly force F_1 or pull-out force F_2 is obtained?

a) Socket opening diameter D_K

According to table 1 the maximum permissible elongation for Hostacom G3 N01 is $\varepsilon_{max.} = 1\%$.

Thus using formula (8)

$$\varepsilon = \frac{D_G - D_K}{D_K} \cdot 100\,\%$$

$$D_K = \frac{D_G}{\frac{\varepsilon}{100} + 1}$$

$$D_K = \frac{8}{0.01 + 1}$$

$$\underline{D_K = 7.92\ mm}$$

b) Assembly force F_1 = pull-out force F_2

For $\varepsilon = 1\%$, table 5 gives a retaining angle of $\alpha_2 = 8°$. The deformation length divided by the ball diameter is $\frac{a}{D_G} = 0.07$ according to table 5.

For Hostacom/Hostacom the coefficient of friction is $\mu = 0.4$ (table 2).

For $\frac{D_a}{D_G} = \frac{14}{8} = 1.75$ for K using formula (26).

$$K = \frac{\left(\frac{D_a}{D_K}\right)^2 + 1}{\left(\frac{D_a}{D_K}\right)^2 - 1} + 1$$

$$= \frac{\left(\frac{14}{7.92}\right)^2 + 1}{\left(\frac{14}{7.92}\right)^2 - 1} + 1$$

$$K = 2.94$$

According to fig. 17 the secant modulus of Hostacom G3 N01 for $\varepsilon = 1\%$ is

$$E_S = 4400\ N/mm^2.$$

The joint pressure can be calculated with $H = D_G - D_K$ from formula (23):

$$p = \frac{H}{D_K} \cdot E_S \cdot \frac{1}{K}\ [N/mm^2]$$

$$= \frac{0.1}{7.92} \cdot 4400 \cdot \frac{1}{2.94}$$

$$p = 18.89\ N/mm^2$$

The assembly or pull-out force is then (formula 25):

$$F_{1,2} = p \cdot \pi \cdot D_G^2 \cdot \frac{a}{D_G} \cdot \frac{\mu + \tan\alpha}{1 - \mu \cdot \tan\alpha}$$

$$= 18.89 \cdot \pi \cdot 8^2 \cdot 0.07 \cdot \frac{0.4 + 0.14}{1 - 0.4 \cdot 0.14}$$

$$\underline{F_{1,2} = 152\ N}$$

6.4 *Barbed leg snap-fit supported on both sides*

The two housing halves of a box-shaped moulding made from Hostacom M2 N01 are to be non-detachably joined by 2 barbed leg snap-fits supported on both sides (fig. 31).

Fig. 31

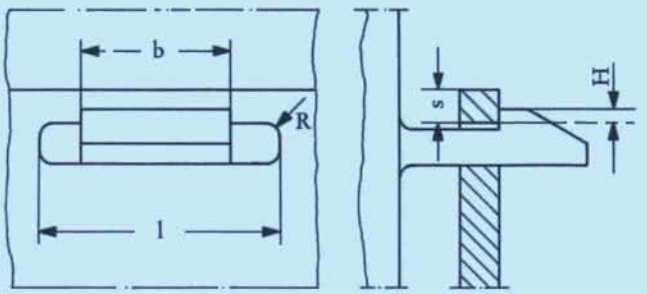

What should the dimensions of the snap-fit joints be?

The receiving holes in the moulding are l = 20 mm.

The maximum permissible elongation $\varepsilon_{max.}$ according to table 1 is

$$\varepsilon_{max.} = 6\,\%$$

The width of the barb is assumed to be b = 8 mm. This gives a barb width ratio of

$$\frac{b}{l} = \frac{8}{20} = 0.4$$

For an assumed spring element thickness of s = 3 mm, a spring element thickness ratio of

$$\frac{s}{l} = \frac{3}{20} = 0.15 \text{ is obtained.}$$

With the aid of fig. 14, an undercut ratio of $\frac{H}{l} = 0.019$ is determined.

The undercut H of the barb is then calculated from

$$H = 0.019 \cdot l$$

$$= 0.019 \cdot 20$$

$$\underline{H \approx 0.4 \text{ mm}}$$

Note:
A possible flow line in the region of the spring element could provide a weak point. By increasing wall thickness at this point, design strength can be improved (see also C.3.4 Guidelines for the design of mouldings in engineering plastics, p. 25, no. 18).

7. *Demoulding of snap-fit joints*

The undercut on which the effect of the snap-fit depends has to be demoulded after injection moulding. The important question here is whether the parts can be directly demoulded or whether it is necessary to bed the undercut in slides, followers or collapsible cores.

There is no general answer to this. The maximum permissible deformation values quoted in table 1 can of course be applied equally well to parts during demoulding. Problems usually arise from the introduction of deformation forces into the component. These can result in local stretching of the part or cause the ejector to press into the part, among other undesirable consequences. A disadvantage here is that the demoulding temperature is considerably above room temperature and hence material stiffness is correspondingly low.

With cylindrical snap-fits, it should be remembered that the dimensional stiffness of a tubular part under compression is greater than under tension. The hub of a snap-fit (fig. 32a) is generally easier to demould than the shaft. In some cases, the parting line of the mould can run through an undercut edge, for example with a through hole and inwardly projecting lip (fig. 32a) or with an outwardly projecting lip (fig. 32b).

In the more frequent case of a blind hole (fig. 33), the inner and outer faces of the undercut must be demoulded in succession. When the mould has opened (A), the cylinder 1 is pressed out of the mould cavity by ejector 3. It takes core 2 along with it until stop 4 is reached (B). Through further movement of the ejector, the cylinder is stripped from the core. Expansion of the hub by an amount corresponding to undercut depth is not prevented (C).

Fig. 32

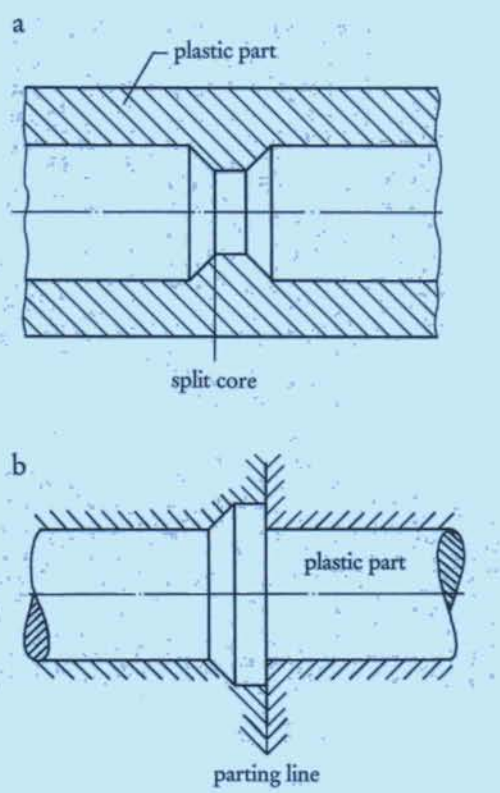

Fig. 33

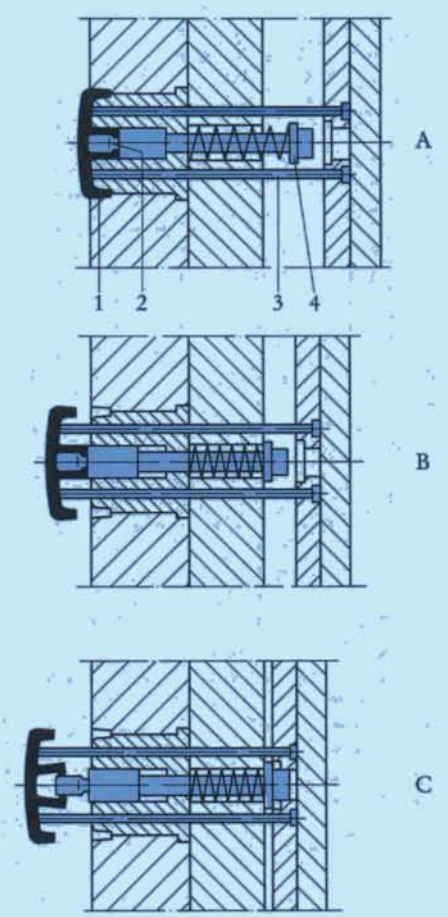

8. *Applications*

8.1 Barbed leg snap-fit

Photo 1 shows examples of snap-fits in which the deformability of the cylindrical snap-fit has been increased by means of slots. In the top half of the picture there are two rollers with Hostaform bearings for dishwashers. In the left roller, each barbed leg is deflected by $f = 0.75$ mm during assembly. With a barbed leg length of $l = 7$ mm and a barbed leg height of $h = 2.5$ mm, the maximum elongation at the vulnerable cross-section of the leg support point is:

$$\varepsilon = \frac{3}{2} \cdot \frac{f \cdot h}{l^2} = 0.058 = 5.8\%.$$

The lower half of the picture shows how a Hostaform bearing bush is fixed. The bush is secured axially at one end by a barbed leg and at the other by a flange. Rotation of the bush is prevented by flattening off the flange.

In all the examples shown, the assembly angle $\alpha_1 = 45°$, the retaining angle $\alpha_2 = 90°$ and the joints are non-detachable.

Photo 2 shows Hostaform fasteners which considerably facilitate assembly, particularly in mass production. Nos. 1, 2 and 3 are used to fix interior trim in cars. No. 4 is a cable holder as used in washing machines and dishwashers. No. 5 is a clip with a similar function. Here the snap-fit is secured by driving a pin into the hollow shank (expanding rivet). The clips for fixing car exterior trim (no. 6) work on the same principle. No. 7 shows the hinge fixing for a detergent dispenser tray flap on a washing machine.

Photo 1

Photo 2

In photo 3 another application from the automotive industry is shown. This is a Hostaform plug box which snap-fits into the fascia panel. The part is made in two symmetrical halves which are inserted into each other.

Photo 4 shows a Hostaform release lever for a car boot lid, which is secured by two pairs of barbed legs.

Photo 5 shows that non-cylindrical housing parts can also be joined by barbed legs. This air filter intake is made from Hostacom G2 N01. In assembling the two halves, the barbed legs are not deflected but the mounting holes are elastically deformed.

Photo 3

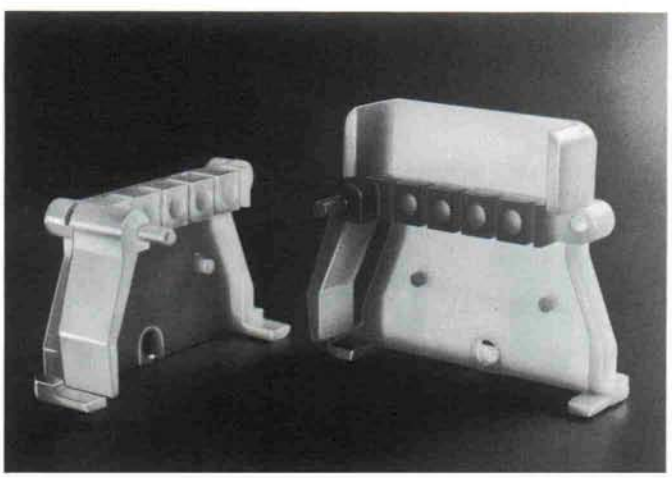

Photo 4

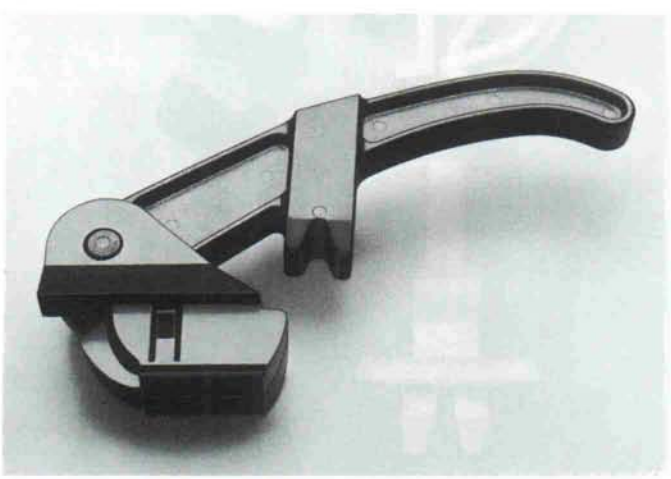

Photo 5

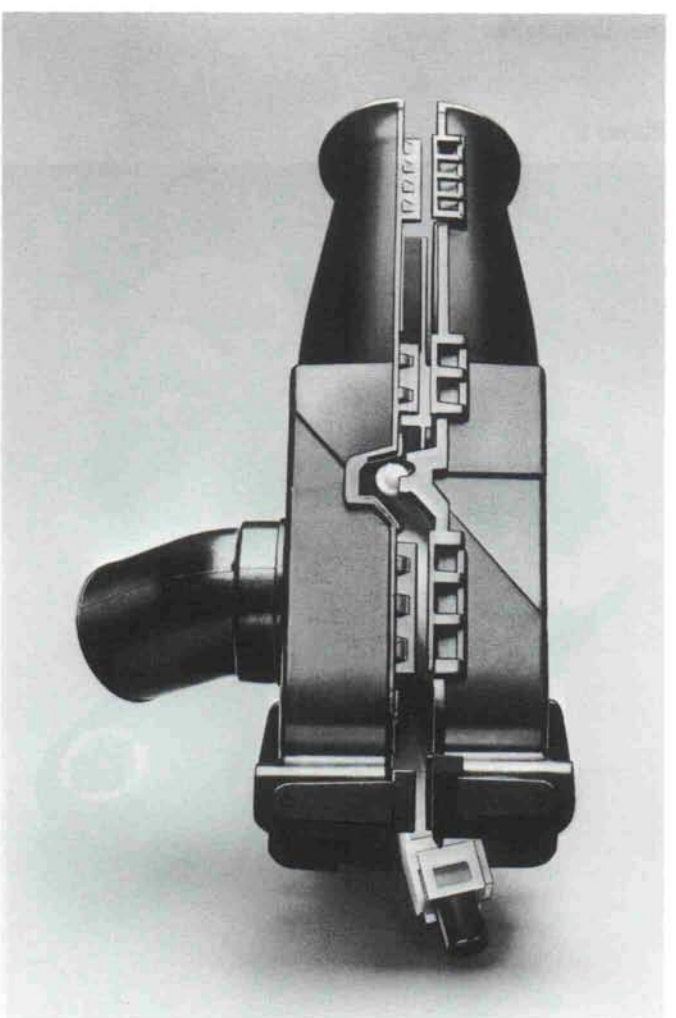

8.2 *Cylindrical snap-fit*

Photo 6 shows a pneumatic positioning device for controlling the flaps in air conditioning systems. The two Hostaform halves are snap-fitted together, thereby at the same time forming a seal by means of an O-ring. The operating pressure is 0.2 to 0.8 bar. The undercut depth is H = 86.5 − 84 = 2.5 mm. Owing to the different wall thickness of the shaft and hub, the hub is extended more than the shaft during assembly. The diameter difference is apportioned between 1.56 mm expansion of the hub and 0.94 mm compression of the shaft.

Photo 7 shows an adjuster for a car, which is similar in design to the previous example. It is controlled by the carburettor vacuum. Here, too, a rubber diaphragm is secured by the snap-fit joint connecting the two halves.

The assembly diameter is $D_G = 60.8$ mm and the undercut depth H = 1.6 mm. Assuming that during assembly only the hub is expanded, the maximum permissible elongation is

$$\varepsilon = \frac{1.6}{60.8} \cdot 100\% = 2.6\%.$$

The assembly angle is $\alpha_1 = 45\,°$ and the retaining angle $\alpha_2 = 45\,°$.

Photo 6

Photo 7

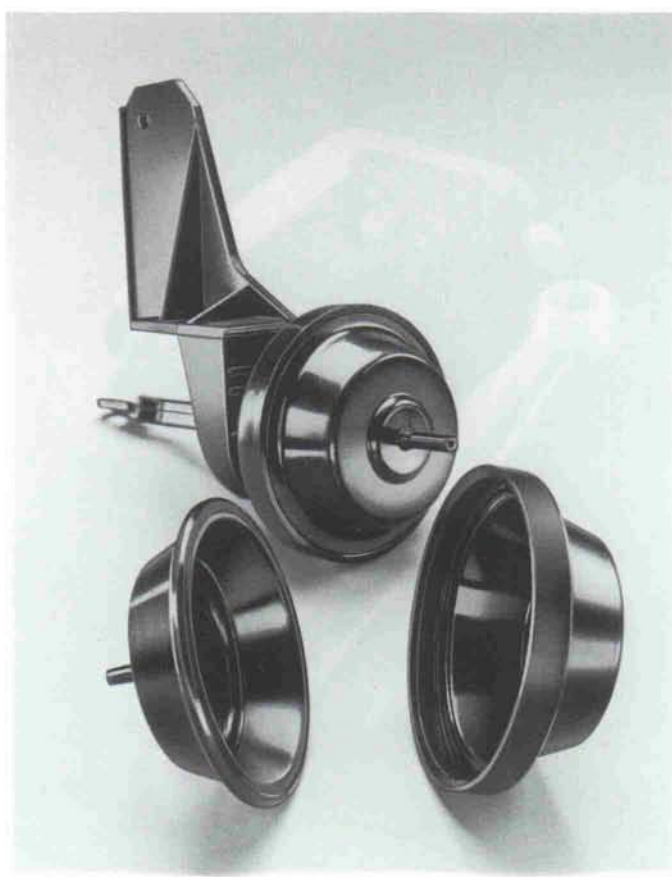

8.3 *Ball and socket snap-fit*

Photo 8 shows parts of a carburettor linkage made from Hostaform. The ball, with a diameter of $D_G = 7.8$ mm, bears in a socket with a diameter of 7.85 mm. The special feature of this design is the socket opening which is not circular but elliptical. The major axis of the ellipse corresponds to the ball diameter $D_G = 7.8$ mm, the minor axis is 7.5 mm in length. In this direction, the diameter difference is

$$H = 7.8 - 7.5 \text{ mm} = 0.3 \text{ mm}$$

Assuming that this diameter difference is spread evenly around the circumference, during assembly the parts will be expanded by

$$\varepsilon = \frac{0.3}{2 \cdot 7.5} \cdot 100 = 2\%.$$

Photo 8

9. *Explanation of symbols*

Symbol	Unit	Explanation
A	mm^2	area
a	mm	deformation length (ball and socket snap-fit
b	mm	barb width (barbed leg snap-fit supported on both sides)
D_a	mm	outside diameter of hub
D_G	mm	largest diameter of the shaft (cylindrical snap-fit)
	mm	ball diameter (ball and socket snap-fit)
D_K	mm	smallest diameter of the hub (cylindrical snap-fit)
	mm	socket diameter (ball and socket snap-fit)
E_s	N/mm^2	secant modulus (fig. 17)
F_1	N	assembly force
F_2	N	pull-out force
h	mm	barbed leg height
H	mm	undercut depth
$H_{max.}$	mm	maximum permissible undercut depth
J	mm^4	moment of inertia (table 3)
K		geometry factor (fig. 26)
$L_1 - L_2$	mm	difference between outside edge of leg and inside edge of hole
l	mm	barbed leg length
	mm	length of receiving hole (barbed leg snap-fit supported on both sides)
p	N/mm^2	joint pressure $p = \frac{H}{D_K} \cdot E_s \cdot \frac{1}{K}$
s	mm	wall thickness
α_1	°	assembly angle
α_2	°	retaining angle
ε	%	elongation
$\varepsilon_{max.}$	%	maximum permissible elongation
$\dot{\varepsilon}$	%/min	rate of elongation
μ		coefficient of friction (table 2)
σ_B	N/mm^2	tensile strength (table 4)
σ_R	N/mm^2	ultimate tensile strength (table 4)
τ_B	N/mm^2	shear strength

10. Literature

[1] H. Schmidt: Fügen durch Schnappverbindungen, VDI-Z, No. 5, 1972

[2] K. Oberbach, D. Schauf: Schnappverbindungen aus Kunststoff, Verbindungstechnik, Nos. 6, 7 and 8, 1977

[3] W. W. Chow: Snap-fit design concepts. Modern Plastics International, August 1977

Engineering plastics
Design · Calculations · Applications

Publications so far in this series:

A. Engineering plastics

- A.1.1 Grades and properties – ®Hostaform
- A.1.2 Grades and properties – ®Hostacom
- A.1.4 Grades and properties – ®Hostalen GUR
- A.1.5 Grades and properties – ®Celanex, ®Vandar, ®Impet
- A.2.1 Calculation principles
- A.2.2 ®Hostaform – Characteristic values and calculation examples
- A.2.3 ®Hostacom – Characteristic values and calculation examples

B. Design of technical mouldings

- B.1.1 Spur gears with gearwheels made from ®Hostaform, ®Celanex and ®Hostalen GUR
- B.2.2 Worm gears with worm wheels made from ®Hostaform
- B.3.1 Design calculations for snap-fit joints in plastic parts
- B.3.2 Fastening with metal screws
- B.3.3 Plastic parts with integrally moulded threads
- B.3.4 Design calculations for press-fit joints
- B.3.5 Integral hinges in engineering plastics
- B.3.7 Ultrasonic welding and assembly of engineering plastics

C. Production of technical mouldings

- C.2.1 Hot runner system – Indirectly heated, thermally conductive torpedo
- C.2.2 Hot runner system – Indirectly heated, thermally conductive torpedo
  Design principles and examples of moulds for processing ®Hostaform
- C.3.1 Machining ®Hostaform
- C.3.3 Design of mouldings made from engineering plastics
- C.3.4 Guidelines for the design of mouldings in engineering plastics
- C.3.5 Outsert moulding with ®Hostaform

Ticona

Performance Driven Solutions™

World-Class Engineering Polymers

- Celanex® thermoplastic polyester (PBT)
- Celcon® and Hostaform® acetal copolymer (POM)
- Celstran® and Compel® long fiber reinforced thermoplastics (LFRT)
- Fortron® polyphenylene sulfide (PPS)
- GUR® ultra-high molecular weight polyethylene (UHMW-PE)
- Impet® thermoplastic polyester (PET)
- Riteflex® thermoplastic polyester elastomer (TPC-ET)
- Vandar® thermoplastic polyester alloy (PBT)
- Vectra® liquid crystal polymer (LCP)

Please consult the nearest Ticona Sales Office, or call the numbers listed above for additional technical information. Call Customer Services for the appropriate Materials Safety Data Sheets (MSDS) before attempting to process our products. Ticona engineering polymers are not intended for use in medical or dental implants.

Contact Information

Americas
Ticona Engineering Polymers
Product Information Service
8040 Dixie Highway
Florence, KY 41042
USA
Tel.: +1-800-833-4882
Tel.: +1-859-372-3244

Customer Service
Tel.: +1-800-526-4960
Tel.: +1-859-372-3214
Fax: +1-859-372-3125

email: prodinfo@ticona.com

Europe
Ticona GmbH
Information Service
Professor-Staudinger-Straße
65451 Kelsterbach
Germany
Tel.: +49 (0)180-584 2662 (Germany)*
+49 (0)69-305 16299 (Europe)**
Fax: +49 (0)180-202 1202

See example below for rate information:
* 0.14 €/min + local landline rates
**0.06 €/call + local landline rates

email: infoservice@ticona.de

Ticona on the web: www.ticona.com

Asia
Celanese (China) Holding Co., Ltd.
3F, China Development Bank Tower
500 South Pu Dong Road
Shanghai, 200120
P.R. China

Customer Service
Tel.: +86-21-3861 9266
Fax: +86-21-3861 9599

email: infohelp@ticona.com

www.ticona.cn

Celanese

Ticona – A Business of Celanese